RSC Advances

ROYAL SOCIETY OF CHEMISTRY

www.rsc.org/advances

Journal Name

ARTICLE

An electrokinetic-combined electrochemical study of the glucose electro-oxidation reaction: effect of gold surface energy

Received 00th January 20xx,
Accepted 00th January 20xx

DOI: 10.1039/x0xx00000x

www.rsc.org/

N. Arjona,[a*] G. Trejo,[b] J. Ledesma-García,[c] L. G. Arriaga,[b] and M. Guerra-Balcázar,[c**]

The glucose electro-oxidation reaction typically involves several steps and it is strongly influence by the crystalline structure. In this paper, gold with typical {111} defects (namely $Au_{\{111\}}$) and gold with defects enclosed in the (200) plane ($Au_{\{200\}}$) were used to determine the effect of the surface energy in the adsorption and electrooxidation of D-(+)-glucose. To this end, an electrokinetic analysis of surface species was made by means of zeta potential (ζ) measurements and was correlated with an electrochemical study. At low glucose concentration (0.1 mM), the system $Au_{\{200\}}$ showed a positive and large ζ value of 261.26 mV related to protons from the glucose dehydrogenation. $Au_{\{111\}}$ presented a negative ζ value of -98.11 mV associated to the glucose chemisorption plus OH^- adsorption from the electrolyte. At a higher concentration (>20 mM) both systems exhibited positive ζ values (from 40 to 60 mV) related to the glucose dehydrogenation because of saturation of the electrical double layer by glucose molecules. Through cyclic voltammetry, it was observed that at low glucose concentration (<20 mM), both materials had preference to oxidation of glucose by-products. However, at higher concentrations, $Au_{\{111\}}$ favors the glucono-lactone oxidation (0.4 V *vs*. NHE); meanwhile $Au_{\{200\}}$ favors the glucose oxidation (-0.43 V *vs*. NHE). Through the electrokinetic analysis, the behavior of $Au_{\{111\}}$ can be related to its affinity toward the chemisorption of glucose molecules, and the $Au_{\{200\}}$, to a weak glucose chemisorption, which allows the desorption of glucose by-products renewing the gold surface for the further oxidation of glucose molecules.

Introduction

Electrocatalysis is a fundamental part in the electrochemical energy conversion area such us fuel cells, batteries and electrolyzers in order to understand the effect of electrocatalytic materials on their performance and hence upgrade them. These materials are complex systems where the resulting performance such as activity, selectivity and/or stability depends on multiple factors.[1] The material facets, surface defects, metal-support interactions, bulk and surface composition, specific surface properties and others are an example of the electrocatalytic complexity.[2-7] Koper et al,[1] mentioned that the preponderant effects can be grouped in structural or electronic effects. Delgado et al,[8] defined the electrokinetic phenomena (EP) as manifestations of the electrical properties of interfaces, which in a practical sense are usually the unique source of information / characterization for those properties. The electrokinetic phenomena are the result from the motion of a pure liquid (or a solution) through a surface where the flow can be driven by an applied potential or by a pressure gradient.[9] Typical EP driven by an applied potential are the electroosmosis and the electrophoresis. Meanwhile, typical EP resulting for a pressure gradient are the streaming potential and the streaming current.[10] Surfaces in contact with a solution can be electrical charged - and as consequence the formation of the electrical double layer- by two ways: I) ionization or dissociation of the surface group, and II) by the surface adsorption of ions in solution.[11] These phenomena can be measured by means of the electrical potential (ψ). Typically, the diffuse double-layer potential (ψ_d) is measured by the colloidal-probe AFM force technique.[12-15] Nevertheless, can be easily measured by streaming potential or streaming current experiments due to in a practical sense the electrical potential (ψ_d) and the zeta potential (ζ) shows almost the same value.[16]

The information obtained from the so-called zeta potential (also called as electrokinetic potential or slip plane potential) is probably the best resource to characterize a metal-solution interface. The magnitude of this parameter strongly depends on four variables: I) the surface nature, II) its charge (as function of pH), III) the electrolyte concentration in the solution and IV) the nature of the electrolyte.[4] Zeta potential measurements usually are obtained to understand the adsorption mechanism of some species as function of some of the four variables before mentioned.[17-19]

The mechanism for the glucose electrooxidation reaction (GOR) has been studied by several authors.[20-23] The GOR shows a complex mechanism due to the multiple numbers of by-products which can be formed. The glucose oxidation

[a] Centro de Investigación y Desarrollo Tecnológico en Electroquímica S. C., Unidad Tijuana, B.C., C.P. 22444, México
[b] Centro de Investigación y Desarrollo Tecnológico en Electroquímica S. C., Parque Tecnológico s/n, Sanfandila, Pedro Escobedo, Qro., C.P. 76703, México
[c] Facultad de Ingeniería, División de Investigación y Posgrado, Universidad Autónoma de Querétaro, Centro Universitario Cerro de las Campanas, Qro., C.P. 76010, México.
*noe.arjona@yahoo.com.mx & wvelazquez@cideteq.mx, Tel: +52 (664) 6602054 ext. 4416 **minbalca@yahoo.com.mx. Tel: +52 (442) 19200 Ext. 65421.

depends strongly in the electrode nature, surface energy, particle size, pH and others.[24] In aqueous medium the two most common isomers of D-glucose are the α-D-glucose and the β-D-glucose in a 37:63 proportion (Scheme 1). Both of these species correspond to the hemiacetal glucose cyclic form.[25] This indicates that glucose in aqueous medium is more stable in its cyclic form than the branched.

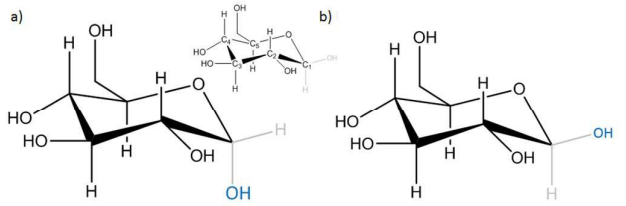

Scheme 1 Forms of the D-glucose in aqueous medium a) α-D-glucose and b) β-D-glucose. Inset: the nomenclature of carbon elements that integrated the glucose molecule

The first step for the electro-oxidation or electro-reduction of any electroactive specie (i.e. formic acid, ethanol, methanol, oxygen, etc.) involves its adsorption on a metal surface. According with the Pletcher theory for the concentric adsorption, the electrocatalytic process involves the hydrogen extraction followed by the simultaneous adsorption of the organic specie (Scheme 2, i.e. glucose adsorption on gold surface).[26] Furthermore, in the case of gold electrodes, it is known that the catalytic component is actually the gold hydroxide (AuOH), which is form by the chemisorption of OH^- anions in the gold surface. Thus, at alkaline pH this effect is more prominent.[27, 28]

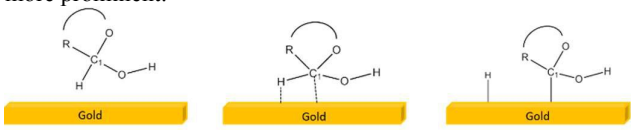

Scheme 2 Pletcher mechanism for the concentric adsorption with adjacent adsorption sites

The OH_{ads} (chemisorbed) has a strong influence in the slow step of the glucose electrooxidation.[28] After the adsorption processes, the dehydrogenated glucose molecule can be oxidized to gluconate or to δ-gluconolactone. It is known that the ratio between these oxidations is influenced by the electrode surface structure. The reaction mechanism -which involves both adsorptions and oxidation- strongly depend on the structure; additionally depends on the glucose concentration and the electrode potential. [27, 28] The dependence on the surface structure manifests dependence on the adsorption sites and in the surface activity.[24] This fact supports the theory of the activation model by chemisorption.

In this work, gold was electrodeposited on glassy carbon electrodes in order to obtain two surfaces with different energies: a gold surface with high (111) defects by cyclic voltammetry and a gold surface with high (200) defects by differential pulse amperometry. D-(+)-glucose adsorption was evaluated in presence and absence of potassium hydroxide commonly used as electrolyte in energy conversion applications through zeta potential values which were obtained by means of streaming potential/current measurements. The effect of the (111) and (200) defects in the glucose adsorption was correlated with the glucose mechanism and therefore, with their effect in the total electrocatalytic activity by cyclic voltammetry experiments.

Experimental

Electrodeposition of gold on glassy carbon electrodes

The electrodeposition of gold surfaces with (111) and (200) defects was previously reported.[29] In brief, a solution composed of 4 mM chloroauric acid ($HAuCl_4$, ≥ 99%, Sigma-Aldrich) as gold ions source and 0.1 M perchloric acid ($HClO_4$, 69.8%, J. T. Baker) as electrolyte was prepared and used as working solution without any surfactant or additive. The electrochemical syntheses were done using a typical glass-jacked three-electrode electrochemical cell through an AutoLab PGSTAT 300 Potentiostat/Galvanostat (Metrohm®). The electrode configuration consisted of glassy carbon plates (20×10 mm, SPI® instruments) as working electrode, the saturated calomel electrode (BAS®, 0.241 V *vs*. NHE) as reference, and graphite plates as counter electrode. All experiments were carried out at 25°C and with an inert nitrogen atmosphere (99.999%, Infra) and were normalized by the Normal Hydrogen Electrode (NHE). Gold with high presence of (111) defects (namely $Au_{\{111\}}$) was synthesized by means of cyclic voltammetry, using a potential window between 0.183 and 1.583 V *vs*. NHE with a scan rate of 100 mV s^{-1} for 20 cycles. Gold with high content of (200) defects (namely $Au_{\{200\}}$) was synthesized by differential pulse amperometry using two pulse potential, a relaxing potential of 1.238 V *vs*. NHE, and a deposition pulse potential of 0.783 V *vs.* NHE, with a pulse duration of 0.1 s, and was repeated for 2500 cycles.

Electrokinetic characterization

The streaming potential/current values were obtained using the Electrokinetic Analyzer for Solid Surface Analysis: SurPASS (Anton Paar®). The adjustable gap cell was used for all experiments; this cell consists in two parallel plates (20×10 mm) where the gap is tuned. The glassy carbon plates were deliberately cut with the 20×10 mm dimensions in order to fit in the adjustable gap cell. The apparent zeta potential (ζ) was determined following the approximation of the Helmholtz-Smoluchowski equation through streaming current (Eq. 1) and streaming potential (Eq. 2) measurements.[30, 31] The streaming potential is related to the specific conductivity of the electrolytic solution. The influence of the surface conductance is taken into account and corrected using the Fairbother and Mastin approximation (Eq. 3).[32]

$$\zeta = \frac{dI}{dP}\cdot\frac{\eta}{\varepsilon_r\cdot\varepsilon_0}\cdot\frac{L}{A} \xrightarrow{L/A=\kappa_B\cdot R} \zeta = \frac{dI}{dP}\cdot\frac{\eta}{\varepsilon_r\cdot\varepsilon_0}\cdot\kappa_B\cdot R \qquad (1)$$

$$\zeta = \frac{dU}{dP}\cdot\frac{\eta}{\varepsilon_r\cdot\varepsilon_0}\cdot\frac{L}{A}\cdot\frac{1}{R} \xrightarrow{L/A=\kappa_B\cdot R} \zeta = \frac{dU}{dP}\cdot\frac{\eta}{\varepsilon_r\cdot\varepsilon_0}\cdot\kappa_B \qquad (2)$$

$$\zeta = \frac{dU}{dP}\cdot\frac{\eta}{\varepsilon_r\cdot\varepsilon_0}\cdot\frac{L}{A}\cdot\frac{1}{R} \xrightarrow{L/A=\kappa_B\cdot R} \zeta = \frac{dU}{dP}\cdot\frac{\eta}{\varepsilon_r\cdot\varepsilon_0}\cdot\frac{\kappa_{0.1}\cdot R_{0.1}}{R} \quad (3)$$

Where (dI/dP) and (dU/dP) are the streaming current and potential, respectively. η is the viscosity, ε_r and ε_0 are the dielectric constant of the solution and the vacuum permittivity, respectively. L, A, R and κ_B are the length of the streaming channel, cross-section of the streaming channel, the DC resistance inside the cell and the ionic conductivity of the working solution, respectively. The gap between the plates is calculated determining the flow rates and the pressure difference measurements through the Hagen-Poiseuille equation (Eq.4); [32, 33] where H is the height of the channel (gap between plates), dV/dt is the flow rate, ΔP is the pressure difference, and W is the width of the streaming channel.

$$H = \sqrt[3]{\frac{12\cdot\eta\cdot L}{W}\cdot\frac{dV/dt}{\Delta P}} \quad (4)$$

D-(+)-glucose (Reagent degree, Sigma-Aldrich) was used for the electrokinetic analysis in the glucose adsorption mechanism. 10 mM potassium hydroxide (87%, J. T. Baker) was used as an electrolyte and hence as OH^- ions source. This concentration was used because at higher concentrations the ionic conductivity strongly affects the streaming current/potential measurements. The potentiometric titrations were made using 0.3 N hydrochloric acid (37%, J. T. Baker) and 0.1 N sodium hydroxide (95%, J. T. Baker). Deionized water (18.4 Ω cm^{-1}, Eccopure®) was further-deionized through a Thermo Scientific Barnstead Easypure II®. The final conductivity of the deionized water was of 0.2 µS cm^{-1}. The streaming current/potential measurements were done at 400 mbar with an electrode gap of 100±2 µm. The working temperature was of 25°C.

Electrochemical characterization

Cyclic voltammetry was used to investigate the effect of the glucose concentration in the electrocatalytic properties of $Au_{\{111\}}$ and $Au_{\{200\}}$ systems. Cyclic voltammograms were obtained using the same electrochemical configuration than that employed for the electrochemical synthesis. 0.3 M KOH (J. T. Baker, 87%) was used instead of 10 mM KOH to avoid the migration contribution. Cyclic voltammetry in acidic media were performed before and after of the glucose electrooxidation experiments as function of glucose concentration in order to determine the electrochemical active surface area (ECSA) and hence normalize the cyclic voltammograms. Also, the cyclic voltammograms in acid media were used to corroborate the presence of the {111} and {200} terraces, the physicochemical evidence of the crystallographic planes and geometry as well as reproducibility and geometry stability can be found in the supplementary information (Figures S1, S2 and S3).

Results and discussion

Electrokinetic characterization

The flow rate *vs*. pressure plots for the system $Au_{\{200\}}$ with glucose (a) and with glucose + 10 mM KOH (b) are shown in Figure 1. The system $Au_{\{111\}}$ exhibited a similar behavior than system $Au_{\{200\}}$, for this reason uniquely $Au_{\{200\}}$ system was discussed. A non-linear flow rate behavior was observed in presence of lower glucose concentration than 10 mM (Fig. 1a, inset) probably due to the poor dissociation of glucose in water. The flow rate trended to decrease with a quasi-linear behavior at higher concentrations than 20 mM. When an electrolyte with good ionic conductivity and high pH value such as 10 mM KOH (242.1 mS cm^{-1}, pH>11) is added to the solution (Fig. 1b), the glucose molecules presented higher dissociation and adsorption in the gold surface (Scheme 2).[28] In this context, when the glucose concentration was increased, the flow rate had a tendency to decrease, which is related to the higher counterions migration from the electrical double layer (EDL) to the end of the channel (in the opposite direction to the pressure-driven flow) by effect of the streaming potential (Fig. 1b, inset). Yang et al,[34] found that at very low concentrations (in the order of 10^{-6} and 10^{-8} M) the flow rate decreases because the strong effect of the EDL. In our case, higher glucose concentrations were used (10^{-4} to 10^{-1} M) where the decrease of the flow rate could be meanly related to ionic-aggregated formation. The EDL effects were depreciated due to the Debye lengths were lower than 30 nm (the electrodes gap was of 100 µm).

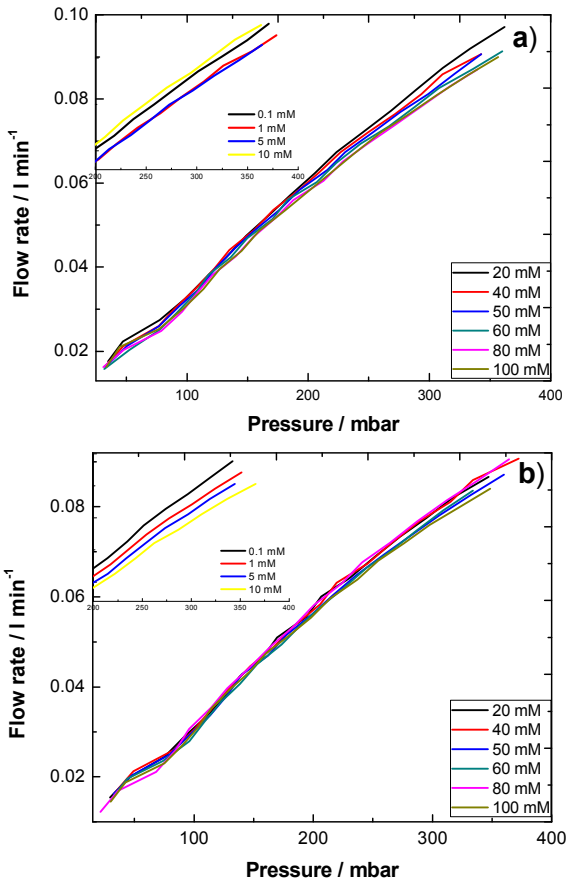

Figure 1 Flow rate vs. pressure plots for the system $Au_{\{200\}}$ as function of a) glucose and b) glucose in presence of 10 mM KOH as basic electrolyte.

The OH^- adsorption from KOH used as electrolyte in both gold surfaces and the effect of glucose at low (0.1 mM) and high concentration (100 mM) in the ζ values of the KOH solution are shown in Figure 2.

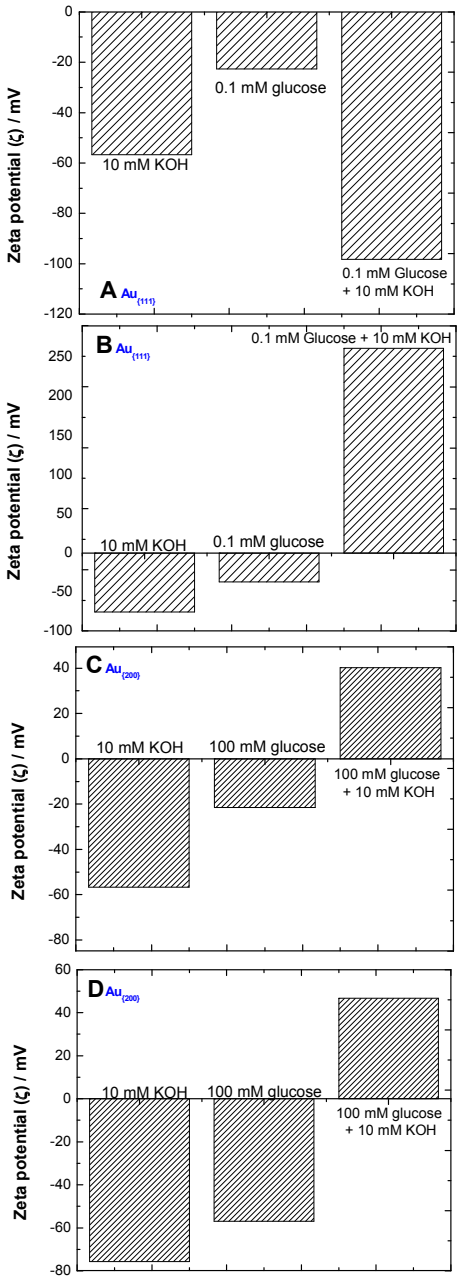

Figure 2 Effect of the electrolyte in Au with {111} terraces at A) the lowest glucose concentration (0.1 mM) and B) the highest glucose concentration (100 mM) and in Au with {200} terraces at C) 0.1 mM and D) 100 mM.

The ζ values in presence of 10 mM KOH and 0.1 mM glucose for the system $A_{\{111\}}$ were of -56.64 and -22.8 mV, respectively (Table 1, Fig. 2A). The resulting zeta potential of [0.1 mM glucose + 10 mM KOH] solution was more negative than their separately components probably due to both OH^- and glucose adsorptions. Increasing the glucose concentration until reach 100 mM in the KOH solution resulted in a positive ζ of 40.18 mV (Fig. 2B, Table 1) despite the negative ζ values of 100 mM glucose and 10 mM KOH. For the system labelled as $Au_{\{200\}}$, the zeta potential value of glucose in water (Table 1) became more negative by means of increasing the glucose concentration probably due to the higher presence of glucose molecules. In the case of 10 mM KOH as electrolyte, glucose at 0.1 mM (261.26, Fig. 2C) showed higher positive zeta potential value than 100 mM glucose (46.69, Fig. 2D).

Table 1 Zeta potential values for $Au_{\{111\}}$ and $Au_{\{200\}}$ under different electrolytic conditions.

Electrolyte	ζ $Au_{\{111\}}$ / mV	ζ $Au_{\{200\}}$ / mV
10 mM KOH	-56.64	-75.75
0.1 mM glucose	-22.80	-38.15
0.1 mM glucose + 10 mM KOH	-98.11	261.26
100 mM glucose	-21.59	-56.98
100 mM glucose + 10 mM KOH	40.18	46.69

Variations in zeta potential values as function of presence of electrolyte and as function of glucose at low and high concentration evidenced changes in the adsorption mechanism, hence the glucose adsorption was investigated in a broader range of glucose concentrations without (Fig. 3a) and with 10 mM KOH as electrolyte (Fig. 3b). Meanwhile, the phenomena resulted from Figure 2 and 3 are illustrated in Scheme 3.

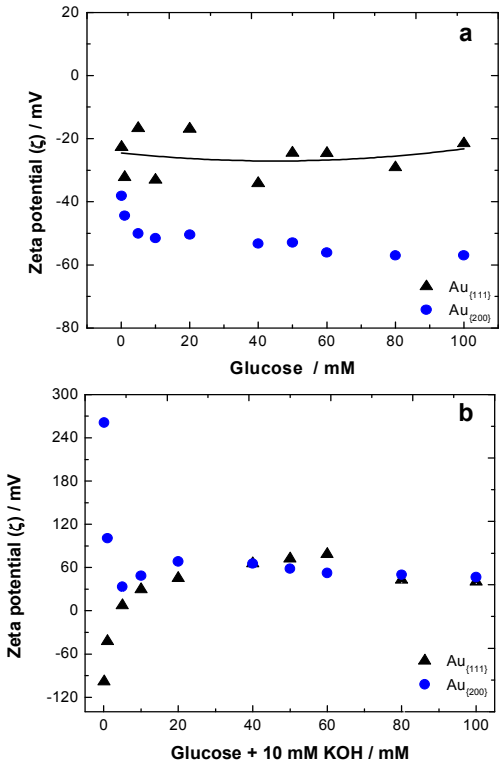

Figure 3 Effect of the glucose concentration in zeta potential of Au with {111} and {200} terraces in a) absence and b) presence of 10 mM KOH.

From the ζ *vs*. glucose concentration (Fig. 3a) two things were observed: first, the ζ reminded negative in all the concentration range for both $Au_{\{111\}}$ and $Au_{\{200\}}$; and two, the $Au_{\{111\}}$ is practically insensitive to the addition and increased of glucose concentration (a smooth line was added in Fig. 3a; the observed small variation were related to experimental deviations). Meanwhile for the $Au_{\{200\}}$ system, the ζ values became more negative with the increased of the glucose concentration. The negative ζ values were related to the oxygen free-electrons (from the hemiacetal OH, Scheme 1) in the glucose adsorption mechanism (Scheme 3b).[35] For $Au_{\{200\}}$ the increase of the glucose concentration promoted a more negative zeta potential due to the chemisorption of a higher amount of glucose molecules. When the glucose was mixed with 10 mM KOH as function of glucose concentration (Fig. 3b) two behaviors were observed: one at low glucose concentration and other at higher concentrations. At concentrations lower than 5 mM, $Au_{\{200\}}$ showed positive ζ values which are related to the presence of {200} defects which promotes the glucose adsorption and its further dehydrogenation instead of OH^- adsorption. The large positive values were a consequence of the $Au_{\{200\}}$ affinity to hydrogen adsorption from the breaking of the glucose molecule (Scheme 3c). The $Au_{\{111\}}$ system showed negative ζ values below 5 mM glucose, which can be related mainly to the OH^- adsorption and to the oxygen free-electrons from the hemiacetal OH in the glucose molecule (Scheme 3d). At higher glucose concentrations than 5 mM both systems showed a similar behavior with positive ζ values. This behavior is related also to the glucose dehydrogenation, where an almost stable positive ζ value was observed due to the saturation of the double layer by effect of the high glucose concentration (>20 mM glucose).

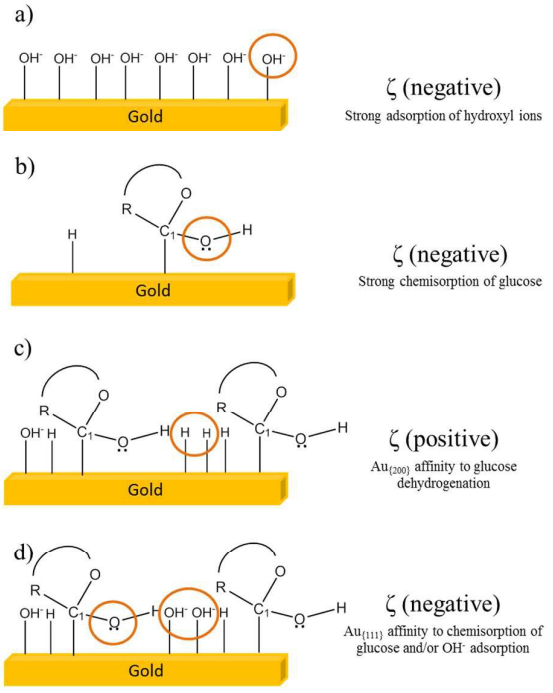

Scheme 3 Representation of the main phenomena that occur in the Au/solution interface by means of electrolyte

ζ *vs*. pH curves were obtained at low (1 mM) and high (100 mM) glucose concentrations using 10 mM KOH as electrolyte in order to evaluate the effect of OH^- and H^+ ions in the glucose adsorption mechanism (Fig. 4).

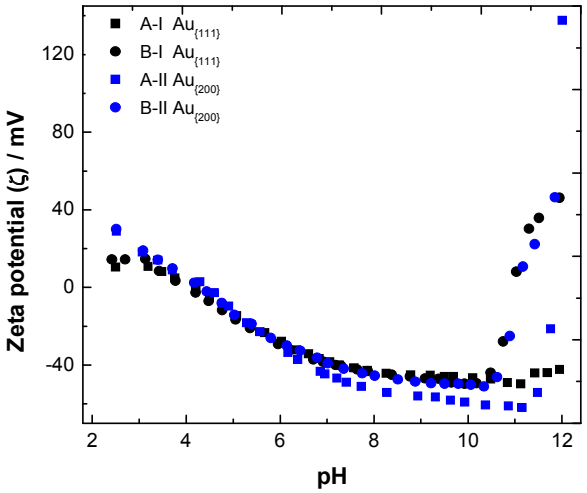

Figure 4 Effect of pH in the zeta potential of Au with {111} and {200} terraces using KOH as electrolyte at 0.1 (A-I and A-II for $Au_{\{111\}}$ and $Au_{\{200\}}$) and 100 mM glucose (B-I and B-II for $Au_{\{111\}}$ and $Au_{\{200\}}$).

Different behaviors were observed at three regions of pH; at high pH (≥11) $Au_{\{200\}}$ exhibits positive ζ values, meanwhile $Au_{\{111\}}$ only showed positive values at high glucose concentration because the high content of glucose molecules in the metal-surface interface, also these results were in concordance with those obtained in Figure 3. A second behavior was observed between pH values of 4.5 to 10, both systems exhibited negative ζ values independently of the glucose concentration. This behavior was associated to the strong chemisorption of glucose, where the negative ζ value could be related to the oxygen free-electrons. In pH below 4.5 both systems ($Au_{\{200\}}$ and $Au_{\{111\}}$) showed positives ζ values related to the H^+ adsorption. In this region the point of zero charge (PZC) was founded at pHs of 4.17 and 4.02 for $Au_{\{111\}}$ at 1 and 100 mM glucose, respectively. For $Au_{\{200\}}$ was founded at pHs of 4.45 and 4.31 for 1 and 100 mM glucose. The shift of $Au_{\{200\}}$ to a relative higher pH than $Au_{\{111\}}$ could be related to the high affinity to H^+ adsorption than glucose adsorption.

Electrochemical characterization

In Figure 5 the electrochemical profiles of $Au_{\{111\}}$ and $Au_{\{200\}}$ are shown. The typical response for Au-based materials was observed. Some differences in the zone of Au oxides formation (1.3 to 1.6 V *vs*. NHE) were observed -and expected- due to the presence of terraces in the gold surface. Three oxidation peaks were located at 1.36, 1.45 and 1.56 V *vs*. NHE, respectively (labelled as I, II and III, respectively). The first peak (Fig. 5A & 5B, peak I) is related to the electro-adsorption of OH^- ions; [21, 36] the second and third peaks (peaks II and III) to the removal of OH_{ads} in order to form gold oxides: AuO and Au_2O_3, respectively. [37, 38] The intensity of the oxidation peaks is related

to specific crystallographic planes, [21] high intensity of the first and second peaks are related to systems with high presence of {111} gold terraces. [29] Meanwhile, high intensity of the third peak is characteristic of systems with high presence of {200} terraces. In this sense, the high presence of {111} and {200} terraces for the systems labeled as $Au_{\{111\}}$ and $Au_{\{200\}}$ was corroborated. The system $Au_{\{200\}}$ showed an intense peak located at 1.06 V, which is attributed to the strong chemisorption of OH^- ions in the Au surface. Meanwhile, for $Au_{\{111\}}$ was not observed. This behavior could be explained with the zeta potential results because of $Au_{\{200\}}$ showed a more negative value than $Au_{\{111\}}$ for the adsorption of OH^- ions. Electrochemical active surface areas (ECSA) were determined through these experiments using theoretical charges of 444 and 384 μC cm^{-2}; [39] which are characteristics for systems with preferential (111) and (100) planes resulting in areas of 0.8470 and 0.4477 cm^2 for $Au_{\{111\}}$ and $Au_{\{200\}}$.

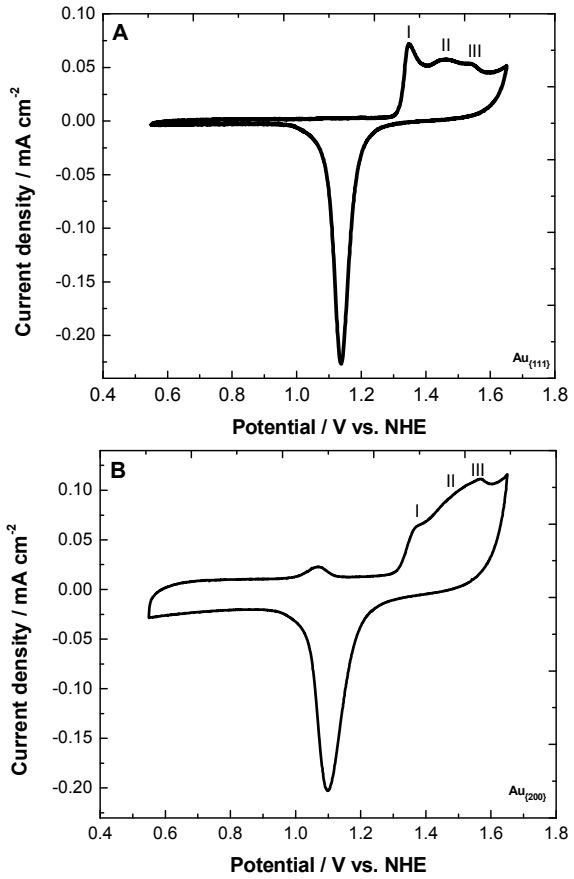

Figure 5 Electrochemical response of Au A) with {111} and B) with {200} terraces in 0.5 M H_2SO_4. Scan rate: 50 mV s^{-1}

The evaluation of the electrocatalytic activity of $Au_{\{111\}}$ and $Au_{\{200\}}$ surfaces for the glucose electrooxidation reaction is shown in Figures 6 and 7, respectively. These graphics were divided in A, B and C for clarity purposes of the effect of glucose concentration. In general, three oxidation peaks were observed and marked as 1, 2 and 3. The first peak or process (Fig. 6 and 7) is related to the oxidation of glucose. [21, 29] The second peak/process to the further oxidation of adsorbed lactone, and the third, to the formation of a gold oxides layer.

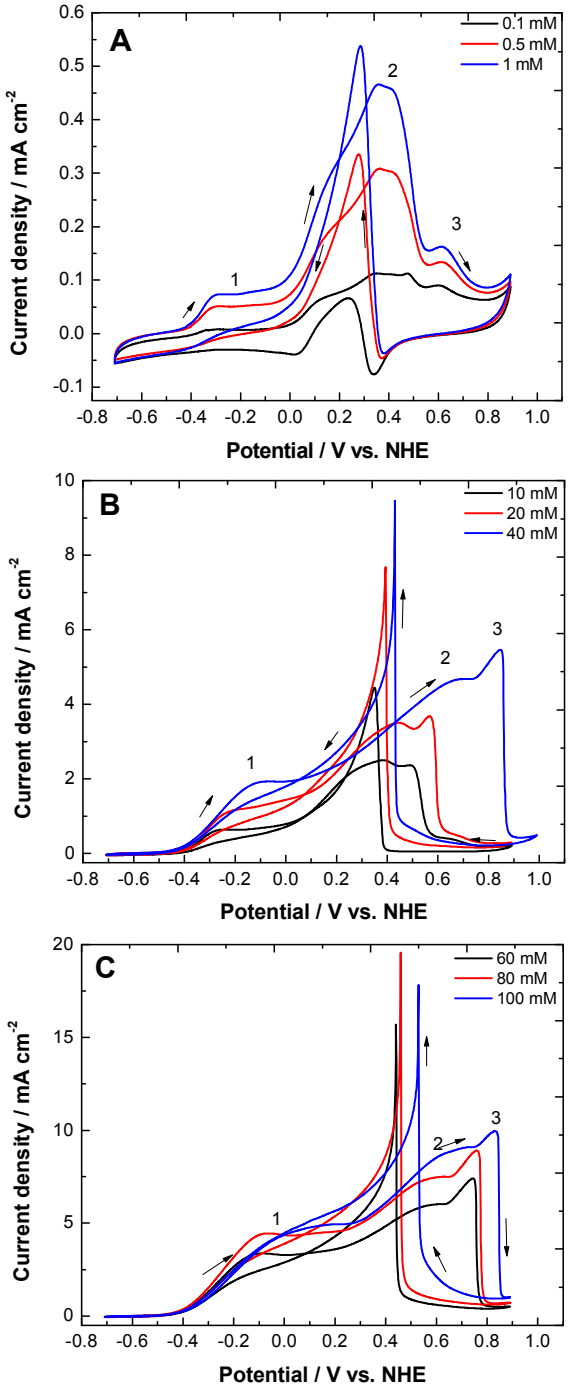

Figure 6 Cyclic voltammograms of the electrocatalytic activity of $Au_{\{111\}}$ toward the glucose electrooxidation reaction in 0.3 M KOH as function of concentration: A) from 0.1 to 1mM, B) from 10 to 40 mM and C) from 60 to 100 mM. Scan rate: 20 mV s^{-1}

An analysis of the effect of gold surface on the reaction mechanism can be done through the values of maximum current density of each process. At low glucose concentrations (from 0.1 to 1 mM), the $Au_{\{111\}}$ surface (Fig. 6 A) in the

positive sweep, showed a 7-fold higher current density of process 2 compared with process 1. Similarly, $Au_{\{200\}}$ surface showed, in the same conditions, a 11-fold higher current density for the process 2 than process 1. These results indicate that both surfaces at low concentrations tend to the oxidation of gluconolactone (process 2) instead of glucose (process 1).

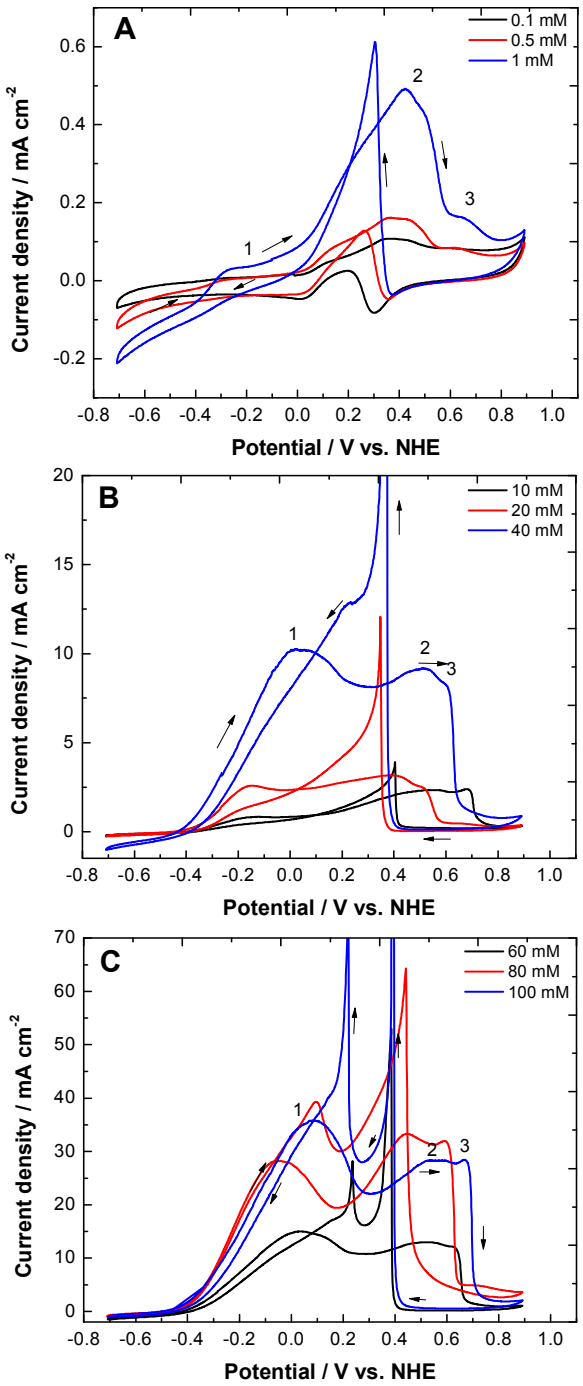

Figure 7 Cyclic voltammograms of the electrocatalytic activity of of $Au_{\{200\}}$ toward the glucose electrooxidation reaction in 0.3 M KOH as function of concentration: A) from 0.1 to 1mM, B) from 10 to 40 mM and C) from 60 to 100 mM. Scan rate: 20 mV s^{-1}

The analysis of current densities at middle concentrations (10 to 40 mM) indicated that, the $Au_{\{111\}}$ surface (Fig. 6 B) still preferred to oxidize gluconolactone. However, the $Au_{\{200\}}$ surface, showed two behaviors. The first, at 10 mM glucose, in which this surface showed higher current density for process 2 than process 1. The second, at concentrations up to 20 mM (Fig. 7 B), at this, the current density of process 1 was slightly superior than process 2, indicating a competition between the glucose and gluconolactone oxidations. When the concentration was increased to 40 mM, the system $Au_{\{200\}}$ preferably oxidizes the glucose molecule instead of its by-products. At higher concentrations (Fig. 6 C and 7 C), $Au_{\{111\}}$ continued oxidizing gluconolactone as well as $Au_{\{200\}}$ still oxidized glucose instead of its by-products.

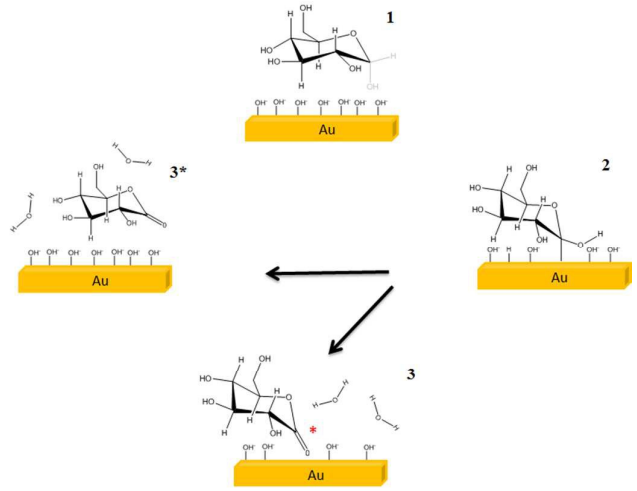

Scheme 4 Limiting steps in the activity of Au-based materials toward glucose electro-oxidation reaction.

An approximation of the glucose electrooxidation mechanism was done linking both, results from the electrokinetic and the electrochemical evaluation (Scheme 4). The mechanism is described as follows: at the beginning, the glucose molecule is deprotonated and adsorbed onto the Au surface (Scheme 4-2). Later, this is oxidized to lactone or gluconolactone (Scheme 4-3). After that, and according with the electrochemical evaluation, two phenomena can occurs: i) the lactone specie is favorably adsorbed on the gold surface, resulting in an increase of the current density of process 2 (Scheme 4-3). And/or ii) the lactone specie is formed and partially removed from the surface (Scheme 4-3*). This capability of gluconolactone of being removed or stay adsorbed, strongly depended on the gold surface. For $Au_{\{200\}}$, the high current density of process 1 was related to the removal of glucose byproducts because of its ability to dehydrogenate glucose molecules. In this sense, the system is continuously renewed which allows a higher oxidation of glucose as was observed in Figure 7 C. In the case of $Au_{\{111\}}$, this surface exhibited affinity to the glucose adsorption (Fig. 2, Scheme 3), therefore glucose and glucose by-products are oxidized and remained adsorbed on the Au surface (Figure 8-3). For this reason, the Au active sites could be blocked avoiding the further oxidation of glucose molecules.

Conclusions

The electrokinetic phenomena are somehow the unique way to characterize the interface between a solid surface and an aqueous electrolyte. Herein, electrokinetic approaches toward glucose adsorption as first step of the glucose electrooxidation reaction, and a further electrochemical analysis to the consecutive glucose oxidation steps were done. For this purpose, two gold surfaces were evaluated: one with defects enclosed in the (111) crystallographic plane and other in the (200) plane.

The adsorption of different electrolytes was analyzed using the determined zeta potential calculated from streaming current values observing that it was strongly influenced by the gold nature probably due to the different surface energy of the $Au_{\{111\}}$ and $Au_{\{200\}}$ systems. D-(+)-Glucose dissolved in water showed negative zeta potential values in both systems due to the adsorption of oxygen free-electrons from the hemiacetal OH in the glucose molecule. Further, 10 mM potassium hydroxide was used as electrolyte and glucose as target molecule concluding that Au with (200) defects showed preference to the hydrogen adsorption instead of glucose, where the H^+ proceeded from the glucose molecule breaking. Meanwhile, Au enclosed in (111) plane showed preference to the glucose adsorption with and without KOH as electrolyte. This behavior modified the mechanism of glucose electrooxidation reaction: $Au_{\{200\}}$ preferred the continuous oxidation of glucose molecules, meanwhile $Au_{\{111\}}$ favored the oxidation of glucose by-products. This can be related with the facility to adsorb or desorb the glucose molecule and the glucose by-products. In summary, the combination of electrokinetic analysis such as streaming current/potential and electrochemical analysis such as cyclic voltammetry is a powerful tool to infer in the reaction mechanism and hence the electrocatalytic activity of electroactive species such as glucose which is highly employed as fuel in the energy conversion area.

Acknowledgements

The authors gratefully acknowledge to the Mexican Council of Science and Technology and the Public Education Ministry for financial support through SEP-CONACYT-2012-01-179921

Notes and references

1 A. S. Bandarenka, M.T.M. Koper, *J. Catal.,* 2013**, 308**, 11-24.
2 R. J. Gillian, D.W. Kirk, S. Thorpe, J. *Electrocatalysis,* 2011**, 2** (1), 1-19.
3 X. Wang, J. Yang, H. Yin, R. Song, Z. Tang, *Adv. Mater*., 2013, **25**, 2728-2732.
4 S. Zhao, H. Yin, L. Du, G. Yin, Z. Tang, S. Liu, *J. Mater. Chem. A*, 2014, **2**, 3719-3724.
5 S. Zhao, H. Yin, L. Du, L. He, K. Zhao, L. Chang, G. Yin, H. Zhao, S. Liu, Z. Tang, *ACS Nano*, 2014, **8**, 12660-12668.
6 H. Yin, H. Tang, D. Wang, Y. Gao, Z. Tang, *ACS Nano*, 2012, **6**, 8288-8297.
7 D. Strmcnik, K. Kodama, D. Van der Vliet, J. Greeley, V.R. Stamenkovic, N.M. Markovic, *Nat. Chem.,* 2009**, 1**, 466-472.
8 A. V. Delgado, F. González-Caballero, R.J. Hunter, L. K. Koopal, J. Lyklema, *J. Colloid Interface Sci.,* 2007**, 309** (2), 194-224.
9 G. Hu, D. Li, *Chem. Eng. Sci.,* 2007**, 62**, 3443-3454.
10 W.B. Zimmerman, *Chem. Eng. Sci.,* 2011**, 66** (7), 1412-1425.
11 M. Zembala, *Adv. Colloid Interface Sci.,* 2004**, 112**, 59-92.
12 J. Drelich, J. Long, Z. Xu, J.H. Masliyah, J. Nalaskowski, R. Beauchamp, Y. Liu, *J. Colloid Interface Sci.,* 2006**, 301**, 511-522.
13 M. Borkovec, I. Szilagyi, I. Popa, M. Finessi, P. Sinha, P. Maroni, G. Papastavrou, *Adv. Colloid Interface Sci.,* 2012, **179-182**, 85-98.
14 M. Finessi, I. Szilagyi, P. Maroni, *J. Colloid Interface Sci.,* 2014, **417**, 346-355.
15 A. Filby, M. Plaschke, H. Geckeis, *Colloids Surf. A. Physicochem. Eng. Asp.,* 2012, **414**, 400-414.
16 M. Giesbers, J. Mieke-Kleijn, M.A. Cohen-Stuart, *J. Colloid Interface Sci.,* 2002**, 248** (1), 88-95.
17 K. Cai, M. Frant, J. Bossert, G. Hildebrand, K. Liefeith, K.D. Jandt, *Colloids Surf., B,* 2006**, 50** (1), 1-8.
18 E.A. Disalvo, A. M. Bouchet, *Colloids Surf. A. Physicochem. Eng. Asp.,* 2014**, 440**, 170-174.
19 M. Markiewicz, W. Mrozik, K. Rezwan, J. Thöming, J. Hupka, C. Jungnickel, *Chemosphere,* 2013, **90** (2), 706-712.
20 A. Martins, V. Ferreira, A. Queirós, I. Aroso, F. Silva, J. M. Feliu, *Electrochem. Commun.,* 2003, **5**, 741-746.
21 M. Pasta, F. La Mantia, Y. Cui, *Electrochim. Acta,* 2010, **55**, 5561-5568.
22 H.-W. Lei, B. Wu, C.-S. Cha, H. Kita, *J. Electroanal. Chem.,* 1995, **382**, 103-110.
23 J. Wang, J. Gong, Y. Xiong, J. Yang, Y. Gao, Y. Liu, X. Lu, Z. Tang, Chem. Commun., 2011, 47, 6894-6896.
24 K.E. Toghill, R.G. Compton, *Int. J. Electrochem. Sci.,* 2010, **5**, 1246-1301.
25 F. Largeaud, K.B. Kokoh, B. Beden, C. Lamy, C. *J. Electroanal. Chem.,* 1995, **397**, 261-269.
26 D. Pletcher, *J. Appl. Electrochem.,* 1984, **14** (4), 403-415.
27 L. D. Burke, *Electrochim. Acta,* 1994, **39** (11-12), 1841-1848.
28 Y.B. Vassilyev, O.A. Khazova, N.N. Nikolaeva, *J. Electroanal. Chem. Interfacial Electrochem.,* 1985, **196** (1), 127-144.
29 N. Arjona, M. Guerra-Balcázar, G. Trejo, J. Ledesma-García, L. G. Arriaga, *New J. Chem.,* 2012, **36**, 2555-2561.
30 C. Bellmann, A. Synytska, A. Caspari, A. Drechsler, K. Grundke, *J. Colloid Interface Sci.,* 2007, **309**, 225-230.
31 A. Yaroshchuk, E. E. Licón Bernal, T. Luxbacher, *J. Colloid Interface Sci.,* 2013, **410**, 195-201.
32 H. Buksek, T. Luxbacher, I. Petrinic, *Acta Chim. Slov.,* 2010, **57**, 700-706.
33 A. Yaroshchuk, T. Luxbacher, *Langmuir*, 2010, **26** (13), 10882-10889.
34 C. Yang, D. Li, J. H. Masliyah, *Int. J. Heat Mass Transfer.,* 1998, **41**, 4229-4249.
35 S. Ernest, J. Heitbaum, C. H. Hamann, *J. Electroanal. chem.,* 1979, **100**, 173-183.
36 H. Angerstein-Kozlowska, B. E. Conway, B. Barnett, J. Mozota, *J. Electroanal. Chem.,* 1979, **100**, 417-446.
37 B. E. Conway, *Prog. Surf. Sci.,* 1995, **49**, 331-452.
38 B. Lertanantawong, A. P. O'Mullane, W. Surareungchai, M. Somasundrum, L. D. Burke, A. M. Bond, *Langmuir,* 2008, **24**, 2856-2868.
39 W. Niu, S. Zheng, D. Wang, X. Liu, H. Li, S. Han, J. Chen, Z. Tang, G. Xu, *J. Am. Chem. Soc.,* 2009, **131**, 697-703.

Table of contents.

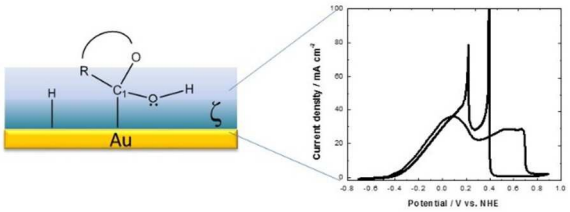

Electrokinetic analysis demonstrate the effect of glucose adsorption on gold surfaces for the glucose electro-oxidation mechanism